

RANSE SIMULATION FOR A TWO DOF SHIP MODEL

Marian RISTEA¹

Adrian POPA²

Alexandru COTORCEA³

¹Assist. prof. PhD, eng. "Mircea cel Batran" Naval Academy, Marine Engineering and Naval Weapons Department

²Assist. prof. PhD, eng., "Mircea cel Batran" Naval Academy, Marine Engineering and Naval Weapons Department

³PhD attendee, "Mircea cel Batran" Naval Academy, Naval and Port Management and Engineering Department

Abstract: *The article shows the results of a CFD study of a PANAMAX tanker which was considered to be placed in head waves, restrained until two degrees of freedom, which corresponds to free heave and pitch motion. The simulation considers several operational draft values. A RANSE (Reynolds Averaged Navier Stokes Equations) solver using finite-volume discretization and free-surface capturing approach is employed for the computation.*

Keywords: AFRAMAX, tanker, RANSE

Introduction

Energy efficiency has become the dominant topic for ship operators especially starting with the moment of MARPOL Annex VI implementation stages. As propulsion accounts for 60-90% (depending on ship type and speed) of the energy consumption of ships, the limelight is on measures to reduce fuel consumption.

Computational fluid dynamics (CFD) is widely seen as a key technology in this respect. CFD denotes techniques solving fluid dynamics equations numerically, usually involving significant computational effort. CFD for resistance and propulsion analyses is sometimes referred to as the "numerical model basin" or the "numerical towing tank".

High-fidelity CFD refers to RANSE (Reynolds-averaged Navier-Stokes equations) solvers which employ fine grids and advanced turbulence models. As high-fidelity CFD requires considerable computational effort and specialized user skills, the industry is looking often for cheaper and simpler alternatives.

The experiment data describing the local flow details are also invaluable in the field of computational fluid dynamics (CFD) for the validation of the developed physical and numerical modeling.

There have been some experimental data for the flows around ship models. The International Towing Tank Conference (hereafter, ITTC) summarized available benchmark database for CFD validation for resistance and propulsion of a ship (ITTC 1999; see also Longo and Stern 1996; Stern et al. 1998). For the cargo-container ship, Series 60 (Fry and Kim 1985; Toda et al. 1990, 1992; Longo et al. 1993; Suzuki et al. 1997) and Hamburg Test Case Bertram et al. 1994; Gietz and Kux 1995) are given. DTMB model 5415 is recommended for a combatant model (Fry and Kim 1985; Ratcliffe 1998; Olivieri and Penna

1999; Longo and Stern 1999). For the full-form tanker, HSVA/Dyne tanker models (Knaack 1992; Denker et al. 1992; Dyne 1995) and Ryuko-Maru (Ogiwara 1994; Suzuki et al. 1998) are given.

Previously, two workshops (Larsson et al. 1991; Kodama 1994) were arranged for the computational analysis of flow around a ship, and HSVA/Dyne tanker models and a Series 60 model were chosen for the test cases. However, those data are often partial and not enough to understand the complicated flow phenomena. The hull forms used in those experiments are old-fashioned and quite different from the modern hull forms of ships today.

Solver

Computation has been performed with the ANSYS CFX solver. Turbulent flow is simulated by solving the incompressible Reynolds-averaged Navier-Stokes equations (RANSE). The flow solver is based on finite volume method to build the spatial discretization of the transport equations. The velocity field is obtained from the momentum conservation equations and the pressure field is extracted from the mass conservation constraint, or continuity equation, transformed into a pressure-equation. In the case of turbulent flows, additional transport equations for modeled variables are discretized and solved using the same principles. The gradients are computed with an approach based on Gauss's theorem.

Non-orthogonal correction is applied to ensure a formal first order accuracy. Second order accurate result can be obtained on a nearly symmetric stencil. Inviscid flux is computed with a piecewise linear reconstruction associated with an upwinding stabilizing procedure which ensures a second order formal accuracy when flux limiter is not applied.

Viscous flux is computed with a central difference scheme which guarantee a first order formal

accuracy. We have to rely on mesh quality to obtain a second order discretization for the viscous term. Free-surface flow is simulated with a multi-phase flow approach. Incompressible and non-miscible flow phases are modeled through the use of conservation equations for each volume fraction of phase/fluid. Implicit scheme is applied for time discretization. Second order three-level time scheme is employed for time-accurate unsteady computation.

Velocity-pressure coupling is handled with a SIMPLE like approach. Ship free motion can be simulated with a 6 DOF module. Some degree of freedom can be fixed as well. An analytical weighting mesh deformation approach is employed when free-body motion is simulated. Several turbulence models ranging from one-equation model to Reynolds stress transport model are implemented in Ansys CFX.

Most of the classical linear eddy-viscosity based closures like the Spalart-Allmaras one-equation model, the two-equation $k-\omega$, SST model by Menter (Menter, 1997), for instance are implemented. Wall function is implemented for two-equation turbulence model.

Description of test case

The test case chosen for the present study is based on an older simulation carried on a TRANSAS LCHS simulator, where for this type of vessel, were determined the loading conditions in several ballast situations. The present case is characterized by a stern draft of 7,56 meters and bow draft of 3,03 meters (Popa I. e.a., 2009), as shown in the following table:

Table 1. Parameters for the simulation (Popa I, e.a. 2009)

Determined value	Load Case		
	I	II	III
Medium draft [m]	2,96	4,77	5,29
Stern draft [m]	5,57	6,32	7,56
Displacement [t]	16500	27896,4	30958
Wetted surface [m ²]	5748,44	6128,89	6163,35
Block coefficient	0,750	0,7871	0,7876

For the considered case, we used several velocities of the current, starting from 10 knots and finalizing with 25 knots.

All calculations described in this paper were conducted for the unappended hull form.

Computational domain

The computational domain was defined for the full scale model, with boundaries at $4 \cdot L_{pp}$ at the stern and aside, and with the inlet boundary at $0.5 \cdot L_{pp}$.

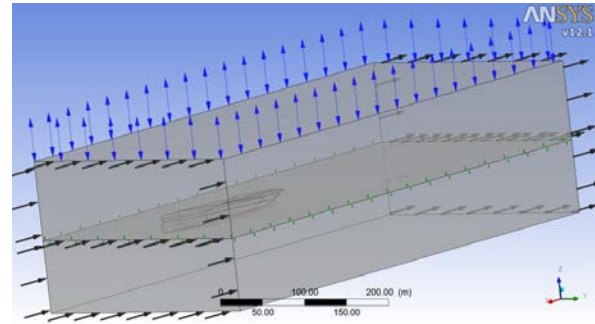


Figure 1. The computational domain

The results presented in this paper were all obtained on unstructured grids with H-O topology and some extra grid clustering close to the ship hull.

Grid studies were conducted using four grids ($m=4$), which enables two separate grid studies to be performed and compared. Grid study gives estimates for grid errors and uncertainties on grid, by using the three finest grids 1-3 while grid study 2 gives estimates for grid errors and uncertainties on grid 2 using the three coarsest grids 2-4. The results for grid study 1 are given in detail and the differences for grid study 2 are also mentioned. The grids were generated using the internal ANSYS code, with consideration to topology; number of points and grid refinement ratio r_G ; near-wall spacing and $k-\omega$ turbulence model requirement that first point should be at y^+

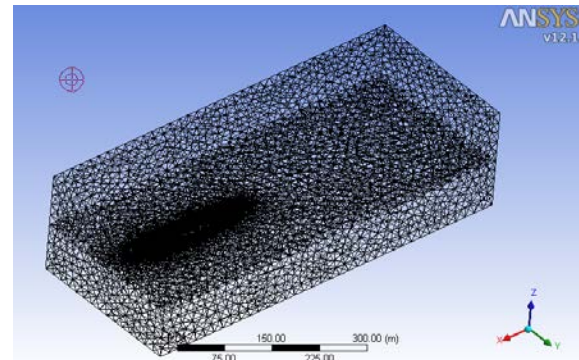


Figure 2. Mesh structure

Table 2. Mesh density

Domain	Nodes	Elements
Air	38341	206321
Water	91131	499955
All Domains	129472	706276

At the ship surface the no-slip condition is applied directly and the normal pressure derivative is assumed to be zero. The undamped eddy viscosity, the variable in Menter’s one-equation model, vanishes at a no-slip wall. With the present formulation of the $k-\omega$ model (Kok and Spekreijse, 2000), all the turbulent quantities are zero at a solid wall.

Numerical Convergence

In the present calculations we have adopted as convergence criterion the reduction of the maximum difference between consecutive iterations of the three velocity components and of the pressure to 10^{-4} .

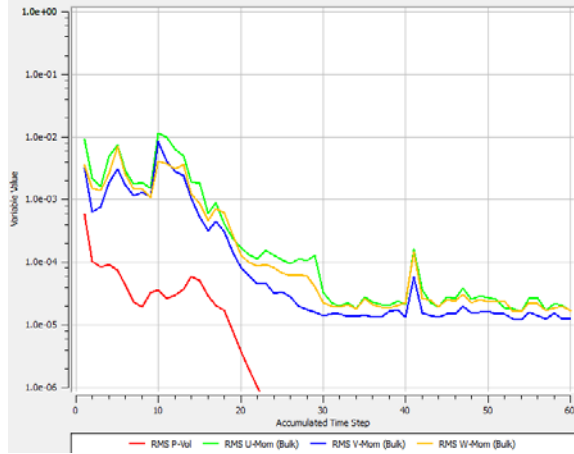


Figure 3. Convergence history

Results

After performing the calculations, there was determined the profiles for pressure and force along the Ox axis and also the velocity profile on the water plane.

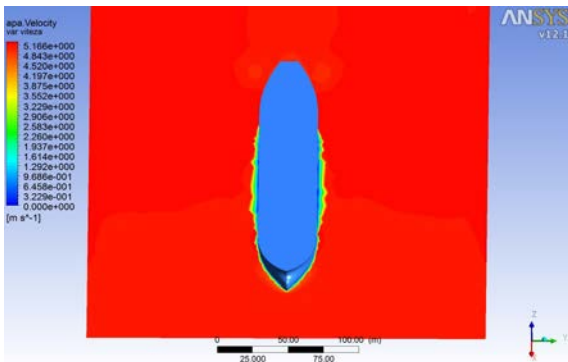


Figure 4. Velocity variation on the free surface plane

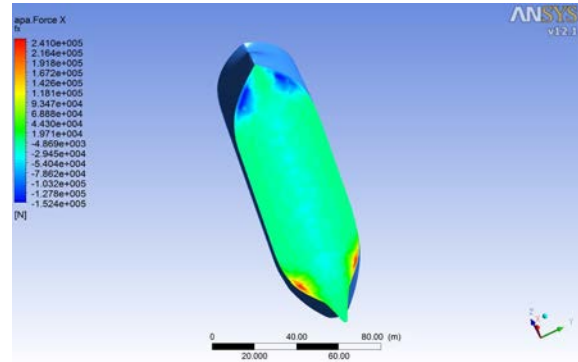


Figure 5. The variation of the drag force along the ship's hull

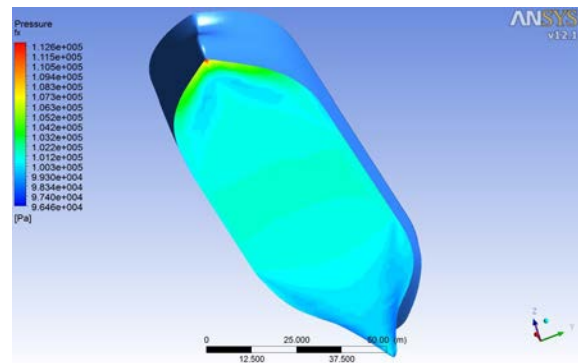


Figure 6. Pressure variation on the ship's hull

CONCLUSIONS

In this paper we focus on the value of the drag force at a certain value of the trim angle and on the variation of pressure along the ship's hull.

It can also be noticed that the maximum values for the force on Ox axis are established in an unusual location, due to the fact that the draft from astern is higher than the one from the bow.

The above depicted results show the fact that the pressure value will be higher in the fore extremity of the bulbous bow, with major pressure drops in the astern area, determined by the stern geometry, which is optimized for a decreased value of turbulences.

The determined values for the drag force are presented in the next table:

Table 3. The drag force

Speed [knots]	Drag Force (-Fx) [KN]
10	396
11	486
12	570
13	668
14	781
15	890
20	1579
25	2480

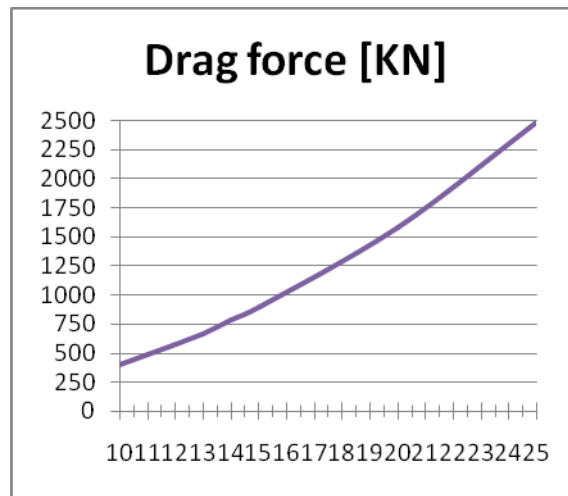


Figure 7. The variation of the drag force

BIBLIOGRAPHY:

[1] Dacles-Mariani J., Zilliac G.G., Chow J.S., Bradshaw P., " Numerical/experimental study of a wing tip vortex in the near field", AIAA Journal, Vol. 33, September 1995, pp. 1561-1568.

[2] Eça L., Hoekstra M., Windt J., "Practical Grid Generation Tools with Applications to Ship Hydrodynamics", 8th International Conference in Grid Generation in Computational Field Simulations, June 2002, Hawaii, USA.

[3] Eça L., Hoekstra M., " An Evaluation of Verification Procedures for CFD Applications", 24th Symposium on naval Hydrodynamics, July 2002, Fukuoka, Japan.

[4] Eça L., Hoekstra M., " A Verification Exercise for Two-D Steady Incompressible Turbulent Flows", 4th European Congress on Computational Methods In Applied Sciences And Engineering, ECCOMAS 2004, July 2004, Finland.

[5] Eça L., Hoekstra M., " On the influence of grid topology on the accuracy of ship viscous flow calculations", 5th Osaka Colloquium on Advanced CFD Applications to Ship Flow and Hull Form Design, 2005, Osaka, Japan.

[6] Kok J.C., " Resolving the Dependence on Free-stream values for the $k - \omega$ Turbulence Model", NLR-TP-99295, July 1999, National Aerospace Laboratory, NLR, The Netherlands.

[7] Kok J.C., Spekreijse S.P., " Efficient and Accurate Implementation of the $k - \omega$ Turbulence Model in the NLR multi-block Navier-Stokes system", NLR-TP-2000-144, May 2000, National Aerospace Laboratory, NLR, The Netherlands.

[8] Menter F.R., " Two-Equation Eddy-Viscosity Turbulence Models for Engineering Applications", AIAA Journal, Vol. 32, August 1994, pp. 1598-1605. Menter F.R., " Eddy Viscosity Transport Equations and Their Relation to the $k - \omega$ Model", Journal of Fluids Engineering, Vol. 119, December 1997, pp. 876-884.

[9] Roache P.J., " Verification and Validation in Computational Science and Engineering", Hermosa Publishers, 1998.

[10] Toxopeus S.L.” Validation of calculations of the viscous flow around a ship in oblique motion”, The First MARIN-NMRI Workshop, October 2004, pp. 91–99.

[11] Popa Ionel, Ristea Marian, Macarie E, Considerations on the Maritime Vessels Ballast Operation, Bulletin of the Transilvania University of Brasov, Vol 2 (51) – 2009 – Series I, Section C, pag 373, ISSN 2065-2119